Solar Energy 153 (2017) 301–316

Contents lists available at ScienceDirect

Solar Energy

journal homepage: www.elsevier.com/locate/solener

Performance analysis and economic assessment of solar thermal and heat pump combisystems for subtropical and tropical region

Yueh-Heng Li [a,b,*], Wei-Chun Kao [a]

[a] Department of Aeronautics and Astronautics, National Cheng Kung University, Tainan 701, Taiwan, ROC
[b] Research Center for Energy Technology and Strategy, National Cheng Kung University, Tainan 701, Taiwan, ROC

ARTICLE INFO

Article history:
Received 10 April 2017
Received in revised form 15 May 2017
Accepted 22 May 2017

Keywords:
Solar collector
Air-source heat pump
TRNSYS
Combisystem
Domestic hot water
Payback period

ABSTRACT

In the present research, combinations of solar collectors and air-source heat pumps for domestic hot water (DHW) are addressed in terms of hydraulic layout and climate conditions. TRaNsient SYstems Simulation (TRNSYS) software was implemented to simulate and examine the heating capacities of various DHW systems. For validating the numerical results, a demonstration site featuring a solar collector and heat pump combisystem with real-time monitoring sensors was established in Tainan, Taiwan. The corresponding parameters of TRNSYS modules were also tested and validated using experimental data. For comparison with the electrical heating water system, three common DHW systems—a conventional solar DHW system, a single-tank solar combisystem, and a dual-tank solar combisystem—were selected, and their technical and economical aspects were assessed. To determine the effect of climate conditions, two metropolitan cities in Taiwan were simulated: Taipei represented subtropical cities and Kaohsiung represented tropical cities. Results for both Taipei and Kaohsiung showed that the dual-tank solar combisystems had the lowest electrical consumption levels and operating costs. The incremental capital costs of the solar combisystems were considered, and realistic payback periods were calculated to determine economic feasibility.

© 2017 Elsevier Ltd. All rights reserved.

1. Introduction

Extensive consumption of fossil fuels leads to irreversible natural resource depletion and increases in carbon dioxide emission. Approximately 81.4% of energy supplied from fossil fuels is consumed for power generation and heating (Chaturvedi et al., 2014). In order to mitigate environmental deterioration, prioritizing the contribution of renewable energy is a timely and urgent issue. Strictly speaking, Taiwan is endowed with almost no energy resources and relies on imports for nearly 98% of its energy consumption (Bureau of Energy, Ministry of Economic Affairs, 2015). Of the imports, 8.3% is nuclear fuel and more than 90% consists of fossil fuels (i.e., petroleum, natural gas, coal). The commercial sector, industrial sector, residential sector, and transportation sector are the four major energy end-use sectors. To confront these challenges, considerable efforts have been undertaken in Taiwan to develop and disseminate renewable energy technologies such as wind energy, solar thermal energy, photovoltaic energy, geothermal energy, biomass energy, and ocean energy (Wu and Huang, 2006; Chen et al., 2008; Chang et al., 2008) The development of solar thermal energy for residential and industrial hot water systems has been particularly widespread. Because of subsidy programs offered by the Bureau of Energy and Ministry of Economic Affairs, the payback period of a solar domestic hot water (SDHW) system is appealing compared with that of an electrical water heating system (Lin et al., 2015).

Recently, combisystems that combine solar collectors and heat pumps for domestic hot water (DHW) systems (Moreno-Rodríguez et al., 2012) and space heating (SH) systems (Xi et al., 2011) have gained increasing consideration for meeting various hot water demands. For SDHW and SH systems, the combination of solar collectors and heat pumps is promising and prevalent in high-altitude regions. The configurations of solar combisystem have been extensively discussed (Liu, 2016; Wang et al., 2010; Buker and Riffat, 2016; Emmi et al., 2015; Liu et al., 2016; Chow et al., 2010). Li et al. (2007) investigated the system performance of a direct-expansion solar-assisted heat pump water heater. Kumar et al. (2016) used artificial neural network (ANN) integrated with genetic algorithm (GA) to predict the performance of direct expansion solar assisted heat pump. Mohanraj et al. (2012) review the applications of artificial neural network (ANN) on different cooling and heating systems. It is noted that the ANN can be successfully applied in heat pump systems. The ANN is a way to applied for

* Corresponding author at: Department of Aeronautics and Astronautics, National Cheng Kung Univ., Tainan 701, Taiwan, ROC.

http://dx.doi.org/10.1016/j.solener.2017.05.067
0038-092X/© 2017 Elsevier Ltd. All rights reserved.

modeling. Qu et al. (2015) examined the effect of hydraulic layout on the system performance of a solar-assisted heat pump water heating system. The results showed that the system with a latent heat storage tank obtained energy performance superior to that of a system with sensible-heat storage. Comparisons of conventional solar thermal systems with solar collectors and heat pump combisystems have indicated that combisystems not only offer superior performance (Buker Mahmut and Riffat, 2016; Carbonell et al., 2014), but also produce much lower CO_2 emissions (Chaturvedi et al., 2014). Lerch et al. (2015) introduced six different configurations of solar combisystems and compared the corresponding performance levels with that of a conventional heat pump system. The solar combisystem appeared to exhibit favorable performance. Although a solar-assisted heat pump can achieve high efficiency, various uncertainties and system factors can influence its overall efficiency and performance, such as compressor speed, solar irradiation, collector area, storage tank volume, and solar collector tilt angle (Hawlader et al., 2001).

Solar collectors can be installed either in parallel or series with a heat pump to manage intermittent solar radiation on a seasonal or daily basis. Consequently, the layouts of solar combisystems can be categorized as series mode layouts and parallel mode layouts (Chu and Cruickshank, 2014). In a parallel system, a solar collector and heat pump provide heat for loads either directly or through a storage system. In a series system, collected heat from a solar collector is used indirectly as a heat source for the heat pump evaporator. In terms of hydraulic connections and system control, parallel systems have the advantage of being less complex than series systems. Therefore, parallel systems may be more robust and reliable (Carbonell et al., 2014). Lund (2005) studied the sizing and applicability of solar combisystems with short-term heat storage, and concluded that large collectors are not suitable for low-energy buildings in regions with high solar irradiation. Li et al. (2014) used TRNSYS software to examine the performance effects of collector areas, storage factors, and dead-band temperatures for air-source heat pump combisystems. Dott et al. (2012) evaluated several configurations of solar collectors and heat pumps regarding the direct or indirect uses of solar irradiation. Poppi et al. (2016) numerically investigated the effects of climate, load, and main components size on electricity use. Panaras et al. (2013) compared the experimental performance of a combined solar thermal heat pump system for DHW with a numerical model and observed favorable agreement for high radiation conditions, but poor agreement for low radiation conditions; they found that the combined solar thermal heat pump system could save approximately 70% of auxiliary energy usage compared with an electric hot water tank. Buker Mahmut and Riffat (2016) curated a number of past and current studies on system design, modeling, and the optimization of the performance characteristics of solar-assisted heat pump systems for low-temperature water heating applications. Haller et al. (2014) used TRNSYS software to estimate the effect of hydraulic integration and the control of a heat pump connected to a solar combi-storage system. The results revealed that unfavorable hydraulic integration causes the system to require additional electrical energy. Kong et al. (2017) developed a mathematical model to analyze the direct-expansion solar-assisted heat pump water heater. Banister and Collins (2015) developed a TRNSYS model and a controller for a dual-tank solar-assisted heat pump. Their system is feasible for application to large loads and produces energy and cost savings. In addition, the effect of climate condition on performance of solar combisystem has been experimentally and numerically discussed in different regions, such as Canada (Asaee et al., 2017; Rad et al., 2013), Denmark (Jradi et al., 2017), Tunisia (Awani et al., 2017), Athens (Tzivanidis et al., 2016), China (Zhu et al., 2015), and Hong Kong (Chow et al., 2010). The climate conditions of these studies pertain cold weather condition or Mediterranean climate, but rarely subtropical and tropical climate. Based on aforementioned literature, many factors would influence the heating performance of solar combisystem. Consequently, the effect of hydraulic layout and climatic condition on the performance of solar combisystem in tropical and subtropical regions will be numerically discussed in this study. Eventually, the incremental capital costs of the solar combisystems were considered, and realistic payback periods were calculated to determine economic feasibility.

2. Validation of DHW system

In this study, commercial TRNSYS 17 software (TRNSYS, 2012) was engaged to analyze the effects of hydraulic layouts on DHW systems and the feasibility of various solar combisystems in Taipei and Kaohsiung. These simulated results were validated with experimental results from a physical solar combisystem. Parameter settings of the solar collector model, such as latitude, longitude, the solar incident angle, and solar radiation, were adjusted to improve the simulation accuracy. For instance, the tilt angle of solar collector can influence the solar thermal quantity. The optimal tilt angle of a solar collector is similar to the latitude in which the system is located (Le Roux, 2016). The validated simulation model was used to assess the performance of various solar systems in Taipei and Kaohsiung, the components and the detailed parameters of solar combisystem were shown in Table 4. Three individual hydraulic layouts were considered in this study, namely a solar combisystem with single tank, a SDHW system, and a heat pump hot water system.

2.1. Experimental setups and simulation model

A lab-scale solar combisystem with real-time monitoring sensors was constructed and tested in Tainan city, the configuration of the experimental apparatus is shown in Fig. 1. The demonstration system consisted of four solar collector panels which are flat-plate type (each of which had an area of 1.92 m^2), two water tanks (each of which held 460 L), two 1-ton storage tanks, and one 1.7 kW heat pump. The working fluid of the heat pump system is R410A. R410A is an environment-friendly refrigerant, and does not contain the chlorine which can cause the damage on the ozone layer. In addition, R410A can achieve much higher performance than traditional refrigerant. Despite of high global warming potential (GWP), R410A is widely used in the world due to its advantages. All water tanks and pipes were thermally insulated to reduce heat loss or gain, allowing the water to be delivered at the intended temperature. K-type thermocouples were used to monitor water temperatures in tanks and pipes. Electromagnetic valves were used to control the water delivery. Flowmeters were used to gauge the water flow rates. Regarding to the environment detection system, a heliograph was used to detect the solar radiation, an anemometer was used to monitor the wind direction and wind speed, and a psychrometer was used to measure the air relative humidity. All data from all sensors were digitally transmitted to and recorded in a computer. Fig. 2 schematizes this solar combisystem and its monitoring sensors. This demonstration system had three configurations corresponding to three types of DHW system. The first configuration acted as a traditional SDHW system, comprising solar collectors and a thermal storage tank. The second configuration acted as a heat pump domestic hot water (HPDHW) system, comprising a heat pump and a thermal storage tank. The third configuration acted as a solar collector and heat pump domestic hot water system (SC-HP DHW), consisting of solar collectors, a heat pump, and a thermal storage tank. These three types of DHW system were simulated in TRNSYS 17; the simulated

Fig. 1. Photograph of the solar domestic hot water demonstration system with environment detection sensors.

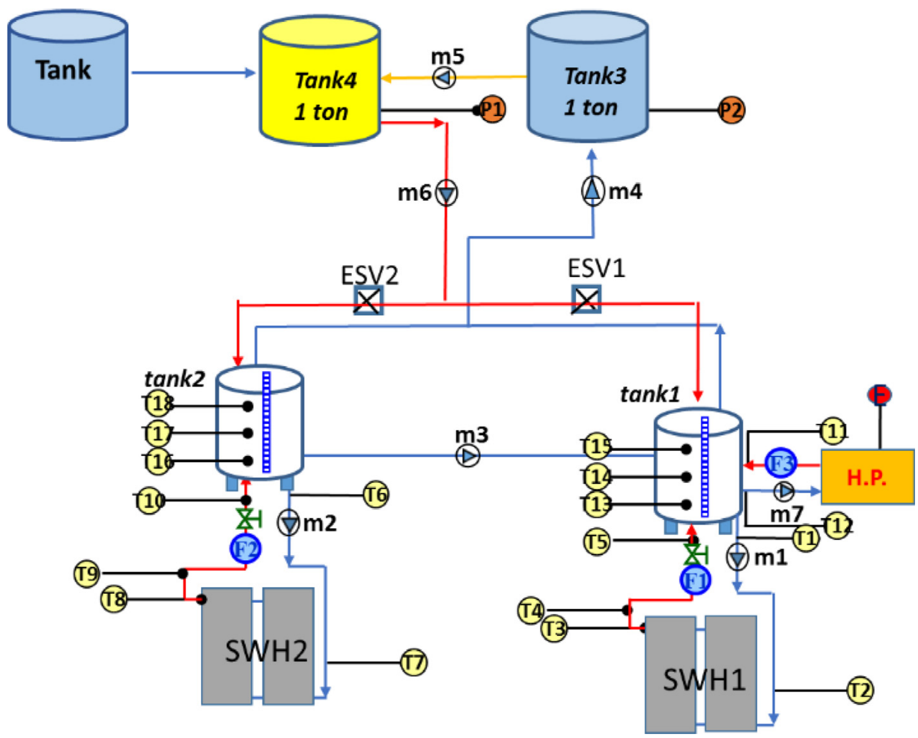

Fig. 2. Schematic of the solar combisystem equipped with sensors.

results were validated with the experimental results. By tuning the parameter settings of certain TRNSYS modules, the simulation was refined; after several iterations, highly accurately parameter settings were obtained. Results demonstrated the feasibility and reliability of using verified TRNSYS models to predict the performance levels of solar combisystems.

2.2. System layout

2.2.1. Solar domestic hot water system

Fig. 3a shows the simulation model and real hydraulic layout of the SDHW system. The SDHW system consisted of two 1.92-m^2 solar collector panels (which collected solar thermal energy and applied it to heat water), a flow meter (which monitored the flow rate), a pump, a valve, and a thermal storage tank without any auxiliary heater. The volume of the thermal storage tank was 460 L, and the valve was used to control the flow rate. In this system, the flow rate was fixed at 4.8 L/min. The pump turned off when the temperature difference between the inlet and outlet of solar collector was below 3 °C, and turned on when the temperature difference was above 7 °C. In the simulation software, many of the models in the standard TRNSYS library were used, including Type 1 (quadratic efficiency collector), Type 3 (pump), Type 2b (controller), and Type 15 (weather data reading and processing). TMY2 is a 10 years meteorological data and it provides statistical climate condition for TRNSYS simulation (Lin and Huang, 2005). Some parameter settings of these TRNSYS models, such as collector area, collector efficiency, flow rate, tank volume, loss coefficient, and weather conditions, were taken from the real system parameters of the physical SDHW and from data measured through sensors monitoring the physical SDHW.

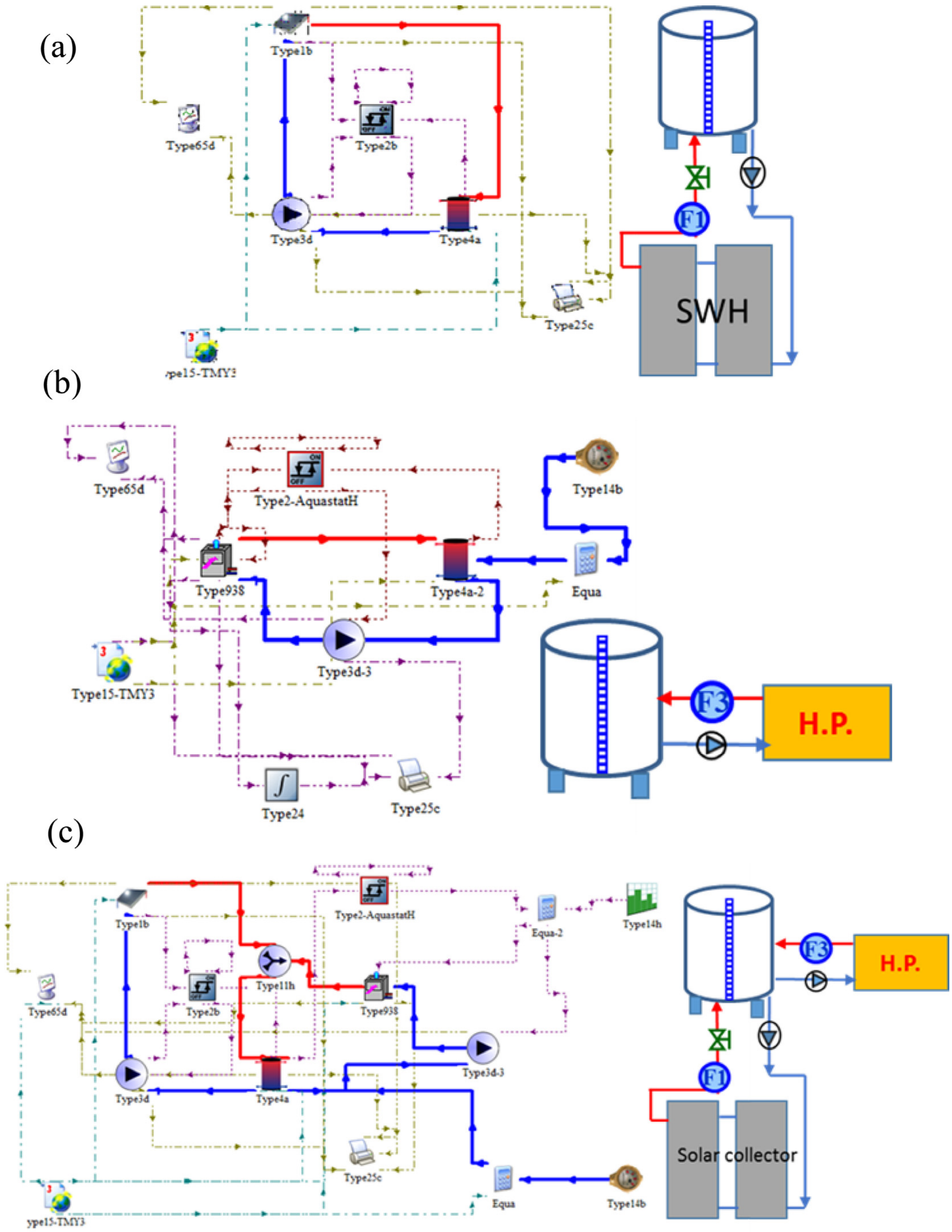

Fig. 3. Solar domestic hot water system (a) SWH system (b) HP system (c) Single tank combisystem.

2.2.2. Heat pump domestic hot water system

Fig. 3b shows the simulation model and real hydraulic layout of the HPDHW system. The four major components of this system were the heat pump, the flow meter, the pump, and the thermal storage tank (which did not have any auxiliary heater). A heat pump with a heating capacity of 7 kW was used to heat water and the flow rate of that heat pump was fixed at 8 L/min. The volume of the thermal storage tank was 460 L. The HPDHW system maintained the following process: water was pumped to the heat pump from the thermal storage tank; the heat pump heated the water; the water moved to the thermal storage tank. The pump turned off when the thermal storage tank temperature reached the thermal set point; the pump restarted whenever the temperature of the water in the thermal storage tank was 5 °C below the thermal set point. The two different heat pump models, Type 938 and Type 941, were tested with this configuration. For Type 941 testing, the effect of relative humidity was not taken into consideration. In general, the effect of relative humidity is expected to influence the heat transfer performance of a heat pump. Therefore, two different heat pump models were engaged to examine the effects of relative humidity on the accuracy of the heat pump simulation under varying climate conditions.

2.2.3. Solar collector and heat pump domestic hot water system

Fig. 3c shows the simulation model and real hydraulic layout of the SC-HP DHW system. This SC-HP DHW system combined parallel flows of hot water from the solar water heating system and hot water from the heat pump. The volume of the thermal storage tank was 460 L. The flow rate of solar collector was fixed at 4.8 L/min and the flow rate of heat pump was fixed at 8 L/min. The main process of this SC-HP DHW system was as follows: water was delivered to the solar collector, heated in the solar collector, and transferred to the thermal storage tank. Whenever the water temperature was below the set temperature, the heat pump turned on and further heated the water. The heat pump used in the simulation model was of Type 938; the humidity effect was calculated because Type 938 heat pumps perform differently at different levels of humidity. This SC-HP DHW system model draws on the SDHW and HPDHW system models.

3. Simulation model descriptions

To quantify the benefits of a combined SC-HP DHW system, a model was developed using TRNSYS simulation software. Three standard systems were compared: a traditional SDHW system, a single-tank SC-HP DHW combisystem, and a dual-tank SC-HP DHW combisystem. The heat pumps installed in SDHW systems are relevant to performance differences between single-tank and dual-tank combisystems. The performance of a combisystem with a heat pump is sensitive to the degree of correlation between ambient temperature and solar irradiation. These systems were modeled using identical weather data. In this study, two cities in Taiwan with similar demographics, lifestyles, and social structures, namely Taipei and Kaohsiung, were compared. Taipei (25°03′N and 121°30′W) is located in northern Taiwan and has a subtropical climate, whereas Kaohsiung (22°38′N and 120°16′W) is located in southern Taiwan and has a tropical climate.

The simulation software was programmed to ensure that all systems had the same delivered water temperature and the same water draw schedule for all configurations. The domestic water (DW) tank in each system was modeled after a 460-L stratified tank. In TRNSYS, each tank was divided into ten nodes of equal size to simulate stratification. An overall uniform loss coefficient of 3 kJ/h m^2 K was applied to each tank; the simulated water was given a specific heat of 4.19 kJ/kg K to simulate real water. The system simulated the 40 °C hot water consumption of a typical four-person family with one-hour water draws at a rate of 300 L/h per person from 9 a.m. to 10 a.m., and one-hour water draws at a rate of 300 L/h per person from 9 p.m. to 10 p.m., for every simulated day. This water draw profile may not be realistic, but it sufficed to draw comparisons.

3.1. System 1: traditional solar domestic hot water system

In a traditional SDHW system, a solar loop augments an electrical water heater. This traditional system comprises a solar collector, a circulating pump, a DW tank with an electric heater, and piping. Whenever the solar loop is activated, cold water from the bottom of the tank is delivered to the solar collector, where it is heated through solar energy, and then it returns to the tank at a higher temperature. If a water draw occurs when the water temperature at the top of the tank is below the desired 50 °C delivery temperature, a 6-kW electric heater is operated to ensure that the water is delivered at the desired set point temperature. In this research, the set point temperature for the electric heater was 55 °C with a dead-band temperature of 5 °C. Therefore, when the water at the height of the thermostat dropped to 50 °C, the heater turned on and remained active until the set point temperature was reached. Fig. 4a shows the hydraulics and the TRNSYS system layout for the traditional SDHW system. A second-order incidence angle modifier flat-plate collector was simulated. TRNSYS constantly calculated the incidence angle modifier throughout the simulation to determine the amount of useful solar energy that was obtained at each specific time point. The area of the collector was similar to the areas in the validating models; the total area of the Type 1b in this scenario was 3.92 m^2. The dominant equation of the collector was derived using the Hottel–Whillier–Bliss equation (Duffie, 1991) with an intercept efficiency of 0.6, an efficiency slope of 6.8, and an efficiencies curvature of 0.4. According to the method of Liu and Jordan (1960), hourly values of total horizontal radiation were categorized into beam and diffuse components. The beam radiation varied with the incidence angle of the collector, and the optimal angle for a collector is approximately equivalent to the angle of latitude at which the collector was installed. According to the latitudes of the targeted cities, each collector was south-facing; collectors were tilted at 25° in Taipei and at 22° for Kaohsiung. The diffuse radiation was assumed to be uniformly distributed with the collector-to-sky view factor. The default values given by the TRNSYS software were used for the coefficients of the quadratic equation; the first-order IAM coefficient was 0.2, the second-order IAM coefficient was 0, and experimental values were used for the other efficiency values, such as the tested flow rate of 72 kg/h m^2.

A Type 3d pump was used to circulate the water at a rate of 100 kg/h; while running, the pump consumed 60 kJ/h of energy and always operated at 100% power. However, the system only

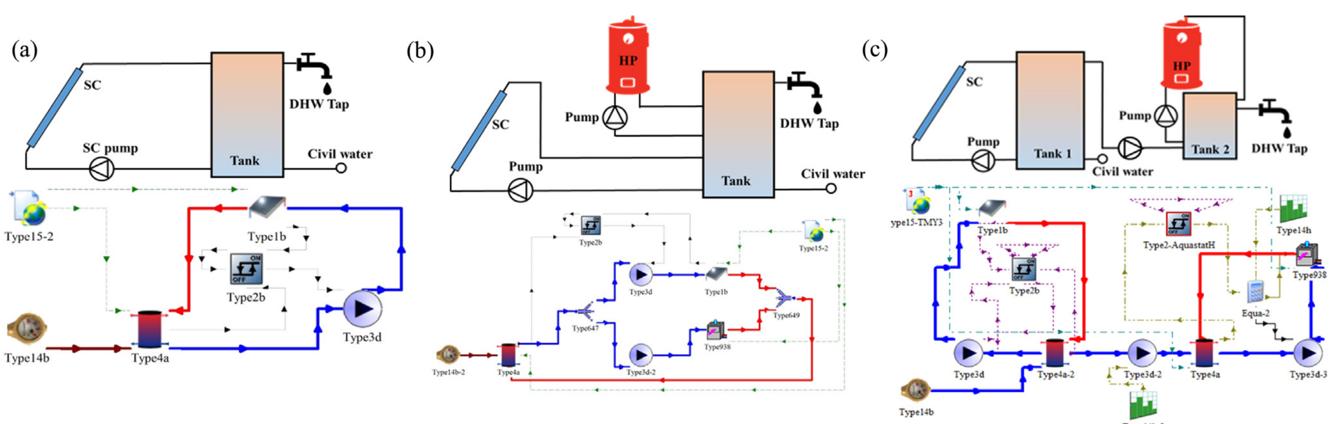

Fig. 4. Layout of SDHW systems (a) SWH system (b) Single tank combisystem (c) Dual tank combisystem.

powered the pump when sunlight added sufficient energy to be collected. TRNSYS simulated a Type 2b differential temperature controller to control the solar loop of the system. It monitored the temperature of the cold water at the bottom of the storage tank and the outlet temperature of the solar collector to determine whether any energy could be collected. If the temperature of the water at the collector outlet is 7 °C or higher than the temperature of the water at the bottom of the tank, the pump was turned on to collect this solar energy. The system continued to operate until this temperature difference fell below 3 °C. The controller also monitored the temperature of the water at the top of the tank and stopped the pump if the water was at 90 °C or higher to prevent the water in the tank from boiling.

Traditionally, an electrical domestic hot water (EDHW) system uses electrical heating in its DW tank to provide all of the energy required to meet load requirements. In System 1 of the present research, the heater turned on when the water at the height of the thermostat fell to 50 °C and remained active until the set point temperature was reached. Therefore, the water in the DW tank never exceeded 55 °C. Unlike the EDHW system, the temperature in the DW tank of the SDHW system in the present research was allowed to rise higher than the required delivery temperature of 50 °C. When the system was able to collect solar energy, the system stored that energy in the DW tank. Accordingly, the temperatures in the DW tank were allowed to be higher than the required delivery temperature of 50 °C. This thermal storage enabled the tank to meet higher load demands when no solar energy was available to heat the tank, and greatly reduced the utilization of the electrical auxiliary heater compared with that of an EDHW system. When solar energy did not suffice to heat the water at the top of the DW tank to the required delivery temperature, the auxiliary heater was used during the water draws to ensure that the water was delivered at 50 °C.

3.2. System 2: solar combisystem with a single tank

A solar loop can be augmented with a heat pump for performance levels exceeding those of a traditional SDHW system. In System 2 of the present research, a solar system was augmented with a collector, a heat pump, a recirculating pump, and piping to produce a single-tank heat pump-assisted solar combisystem. The system hydraulics and TRNSYS layout are shown in Fig. 4b. Two heating loops operated in this system: an SDHW subsystem and a heat pump hot water subsystem. However, the heat pump turned on when the water at the height of the thermostat fell to 50 °C, or during allotted times on a schedule, namely from 8 a.m. to 10 a.m. and 8 p.m. to 10 p.m.

The heat pump used in the TRNSYS model was a Type 938 air-to-water heat pump. An external file determined the energy characteristics of the heat pump. The profile consisted of two inlet water temperatures, two air temperatures, and two air-relative humidity levels; the profile generated a table that determined the power consumption, heating capacity, and cooling capacity levels for all combinations of these values. Other operational points were determined through linear interpolation from this data. The two inlet water temperatures were 9 °C and 15 °C, the two inlet air temperatures were 7 °C and 20 °C, and the two air-relative humidity levels were 58% and 80%. The heat pump model read the input load and source temperatures and then used the external file to determine the power consumption and the energy transfer. In this system, the rated heating capacity of the heat pump was 7 kW, and its power was 1.7 kW.

Two separate loops required control: the solar loop and the heat pump loop. The solar loop was controlled in the manner of a traditional SDHW system. Therefore, when the outlet temperature of the collector was 7 °C higher than the temperature of the water at the bottom of the tank, the pump in the solar loop was turned on. The second loop was the heat pump that supplied energy to the DW tank. The heat pump loop was turned on when the water at middle of the DW tank fell below 50 °C, and remained active until the water had been heated to the set point temperature, 55 °C. This arrangement ensured that the DW tank was constantly charged and able to supply various water draws.

3.3. System 3: solar combisystem with dual tanks

The combination of a solar collector and a heat pump with a single tank causes the two heat sources to compete during the day. Theoretically, the heating capacity of a solar thermal collector capitalizes on temperature differences between inlet water and the absorption plate. The increased temperature of inlet water that had been heated by a heat pump before it entered the solar thermal collector, reduces the solar energy collection capacity of the solar thermal collector. Therefore, the use of a heat pump reduces the contribution of solar energy in this type of DHW system. Separating a storage tank for the solar collector from the DW tank can mitigate this influence. Two separate subsystems operate in this type of combisystem. Fig. 4c shows the system hydraulics and TRNSYS layout for the dual-tank system in the present research. The solar loop was controlled in the same way as in a traditional SDHW system without an auxiliary heating unit. When the outlet temperature of the collector was 7 °C higher than the temperature of the water at the bottom of the tank, the pump in the solar loop was turned on. The collected energy was stored in the storage tank (labeled "Tank 1" in Fig. 4c). In the second loop, the heat pump was used to provide energy to the smaller DW tank (labeled "Tank 2" in Fig. 4c). The same Type 2b controller was used for the heat pump, and the arrangement resembled that of the solar combisystem with a single tank. A pump with a power of 60 kJ/h was able to move water from the storage tank to the DW tank. Cold civil water was fed into the storage tank, and the outflow of the storage tank was pumped into the DW tank.

Characteristically, a solar combisystem with dual tanks can reduce the heating competition between two heating sources during the day, and can reduce the heating load on its heat pump during the night because of its relatively small DW tank. However, the second tank in a dual-tank solar combisystem increases incremental costs and complicates heat loss issues. The electricity consumption levels and operating costs of these three DHW systems were calculated to gauge the realism of these designs and to identify the optimal system. Generic inputs were consistently used with all of the TRNSYS components and the general trends of the results were regarded as more persuasive than the actual numerical values obtained.

4. Results and discussion

Given an accurate simulation model, in which the numerical results are consistent with the physical experimental results for all three DHW systems, one can predict and optimize the performance of a solar combisystem in terms of hydraulic layout and climate conditions. To evaluate the system performance, two indicators were introduced in this study: the seasonal performance factor of the system (SPF) (Kjellsson et al., 2010; Bertram, 2014) and the solar fraction (SF) (Sterling and Collins, 2012; Deng et al., 2013; Reda, 2017). Seasonal performance levels can be calculated to assess the time-dependent performance levels of energy systems under changing operational conditions over a certain time span, usually one year. By accumulating the performance measurements under various operational conditions for an entire year, the overall efficiency can be estimated. Accordingly, the SPF in the present work was defined as the ratio of total thermal energy produced and total electrical energy consumed. The SF was defined as the fraction of solar input to the tank to the total input to the tank: SF = (Energy provided by solar collector)/(The total heat addition by the system). The SF values demonstrated the contribution of renewable energy to these solar collectors in the context of system configuration, hydraulic layout, and climate issues.

4.1. Results of validation system

The results of simulations and experiments for the three DHW systems are compared and discussed in this section. The SDHW system was operated from 8:00 a.m. to 16:00 p.m. Fig. 5 illustrates the numerical and experimental results of solar thermal energy collected by the SDHW system. For both experimental and numerical data, the trends of solar thermal energy collected by the SDHW systems coincided with the distribution of solar irradiation. In Fig. 5a, the default values given by the TRNSYS software were used for the parameter settings of the SDHW system, such as intercept efficiency (0.7), efficiency curvature (0.05 kJ/h m^2 k^2), loss coefficient of solar collector (13 kJ/h m^2 k), and the initial temperature of the thermal storage tank (25 °C). Despite of similar tendency, the simulated results are not consistent with the experimental results. For improving the accuracy of simulated results, these parameters were tailored to certain values, such as intercept efficiency (0.6), efficiency curvature (0.4 kJ/h m^2 k^2), loss coefficient of solar collector (6.8 kJ/h m^2 k), and the initial temperature of the thermal storage tank (20 °C). Apparently, Fig. 5b shows that the average accuracy of numerical results increases 18.55% after adjusting the parameters of TRNSYS modules. The most improvement of accuracy of numerical results occurs in the time period of 11:00 am to 15:00 pm.

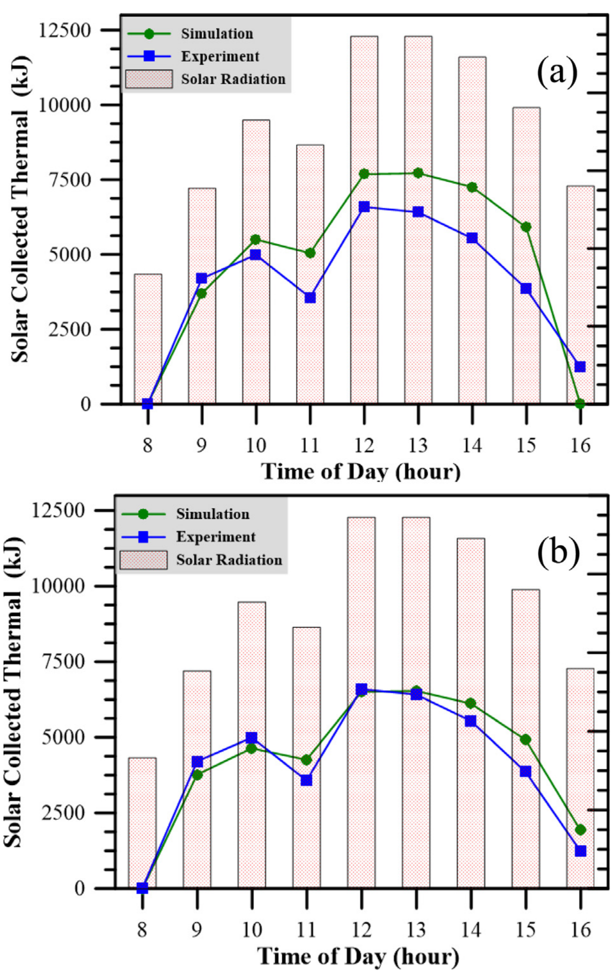

Fig. 5. Solar collected thermal energy values from numerical simulation and experimental demonstration (a) default parameter settings, (b) adjusted parameter settings.

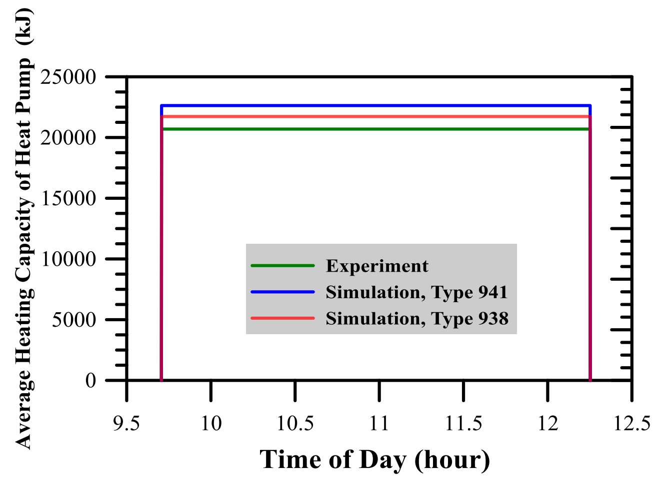

Fig. 6. Average heating capacity of heat pump according to numerical simulation and experimental demonstration.

Fig. 6 compares the average heating capacities of heat pumps in three cases: simulation with the Type 941 module, simulation with the Type 938 module, and experiment with an actual heat pump. The Type 938 simulated results match experimental results more accurately than the Type 941 results do. In the Type 938 case, the effect of relative humidity on heat transfer is taken into consideration. Consequently, simulation with the Type 938 module is relatively more reliable and accurate.

Regarding the simulated and physical SC-HP DHW systems, Fig. 7 shows the quantities of solar thermal energy collected by the solar collectors and the heating capacity values of the heat pumps. All parameter settings for TRNSYS modules were verified through previous individual tests. The shaded areas indicate the periods of hot water consumption. According to the numerical results of Fig. 7, heat pumps ran during three time periods when water temperatures were low, and shut down when the water temperatures of thermal storage tanks achieved the correct temperature. Results indicated a notable interference between solar collectors and heat pumps in single-tank systems that impaired heating performance. Because use of a heat pump increases the temperature of water in a thermal storage tank, use of a heat pump reduces solar thermal utilization in a solar collector. In any such system, a proper heating schedule must be established for heat pump use to avoid competition between the solar collector and the heat pump.

4.2. Influence of water tank deployment

Single-tank designs and dual-tank designs are two distinct types of DHW systems. The water tank volume is associated with the overall efficiency of a DHW system. The larger the tank volume is, the more time the system requires to heat or cool the fluid. If the water tank is too small and solar energy is not available, the temperature fluctuations are drastic and the system cannot meet a high demand without the use of excessive electrical input.

In the hydraulic layout of a dual-tank combisystem, however, the larger storage tank is used to store hot water heated by the solar collector, whereas the smaller DW tank is used to supply

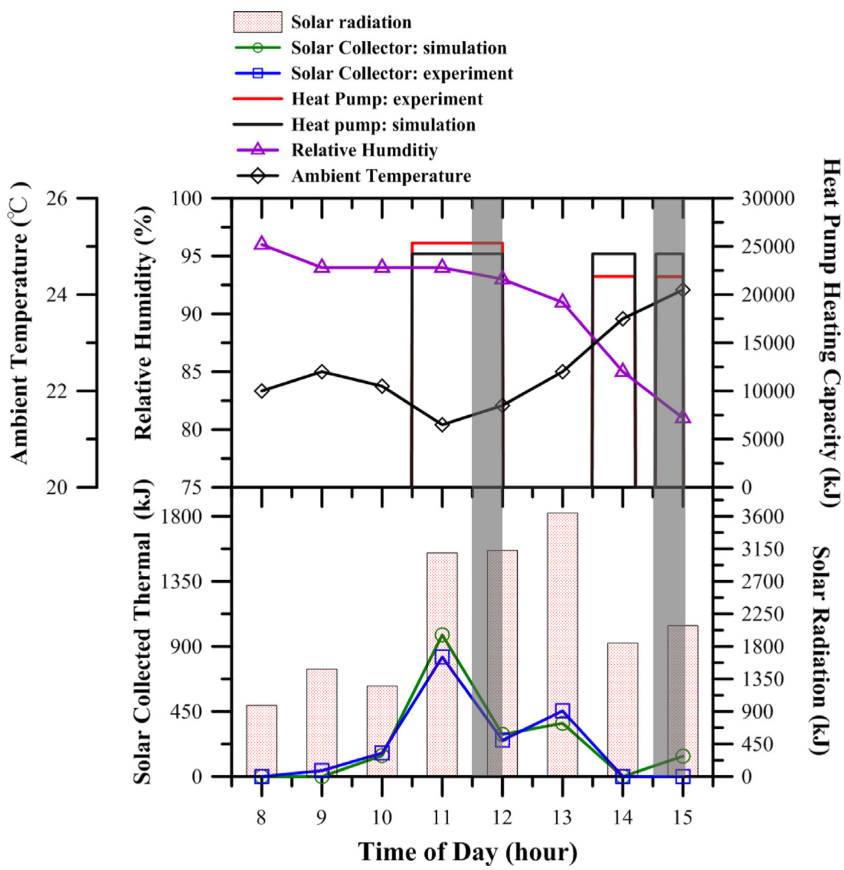

Fig. 7. Heat transfer of solar collector and heat pump domestic hot water system.

the DHW load and is heated by the heat pump. The volume of the storage tank is fixed at 600 L, which is similar to the volume of the DW tank in a SDHW system without a heat pump and the volume of the DW tank in a single-tank SDHW combisystem. The volume of the DW tank in a dual-tank combisystem is associated with the SPF and the water delivery temperature. Fig. 8 presents the SPF and the outlet temperature values corresponding to loads of various volumes in Taipei during January, March, June, September, and December. The DW tanks with small volumes neither can hold sufficient hot water to meet demand nor can deliver adequate water at an appropriate temperature, especially during cold months such as January, March, and December, resulting in additional electrical consumption by the heat pump to compensate for the intermittent supply of solar energy. For this reason, the SPF of such a combisystem declines in cold months. In addition, the temperature of water at the outlet moving to the load also declines in cold months. Electricity consumption depends on the tank volume; a large DW tank can store sufficient hot water and supply the water draws scheduled during the simulation period. However, because a large DW tank requires considerable heat to increase the water temperature, a combisystem with a large DW tank consumes considerable electrical power. A large DW tank provides substantial thermal mass for the combisystem, and the system is able to collect and store considerable solar energy during warm months. By contrast, when solar energy is inadequate, the water in a large DW tank demands considerable DW heating. In addition, the larger a DW tank is, the more heat is lost. To maintain a DW tank at an appropriate water delivery temperature throughout the entire year, the heat pump must compensate for the heat lost from the DW tank. Correspondingly, increasing the size of the DW tank increases the electrical consumption and annual operating costs as shown in Fig. 9. For tank volumes within the simulated range of values, as the volume increases, the monthly seasonal performance and outlet temperature to load both decrease. The fluctuation of outlet temperature to load against various tank volumes is remarkably notable in January. The lowest outlet temperatures occur in January and the corresponding civil water temperature is 40 °C. Accordingly, the proper volume of a DW tank must be larger than 150 L. For a given combisystem, the larger the tank volume is, the lower the SPF is. The minimal acceptable SPF in Taipei is 3.75. Therefore, the most appropriate volume of a DW tank in Taipei is from 150 L to 230 L, as indicated by dark gray shaded area in Fig. 8. In addition, the flow rate of the heat pump is also associated with the heating performance of the combisystem. Fig. 10 shows the monthly SPF values for combisystems of various heat pump flow rates in Taipei during different months. Fig. 11 shows the yearly SPF values for combisystems of various heat pump flow rates in Taipei. SPF values decrease in cold months such as December and March, owing to additional electrical consumption by heat pumps to compensate for the intermittent supply of solar energy. In Taipei, the yearly SPF achieves its highest value when the flow rate of the heat pump is 75 kg/h. However, a heat pump may shut down because of excessively high water temperatures when the flow rate of that heat pump is smaller than 125 kg/h. In Taipei, an appropriate heat pump flow rate is 300 kg/h.

Fig. 12 presents the SPF and the outlet temperature to load for tanks of various volumes in Kaohsiung during different months. The results demonstrate that the SPF of a combisystem in Kaohsiung is higher than that of a comparable combisystem in Taipei. Notably, the values of SPF decrease and the values of outlet temperature to load increase when the tank volume increases. The outlet temperature to load does not reach 40 °C in Kaohsiung in January, when the tank volume is lower than 170 L, and the acceptable minimum of SPF in Kaohsiung is 4.0. To compromise regarding

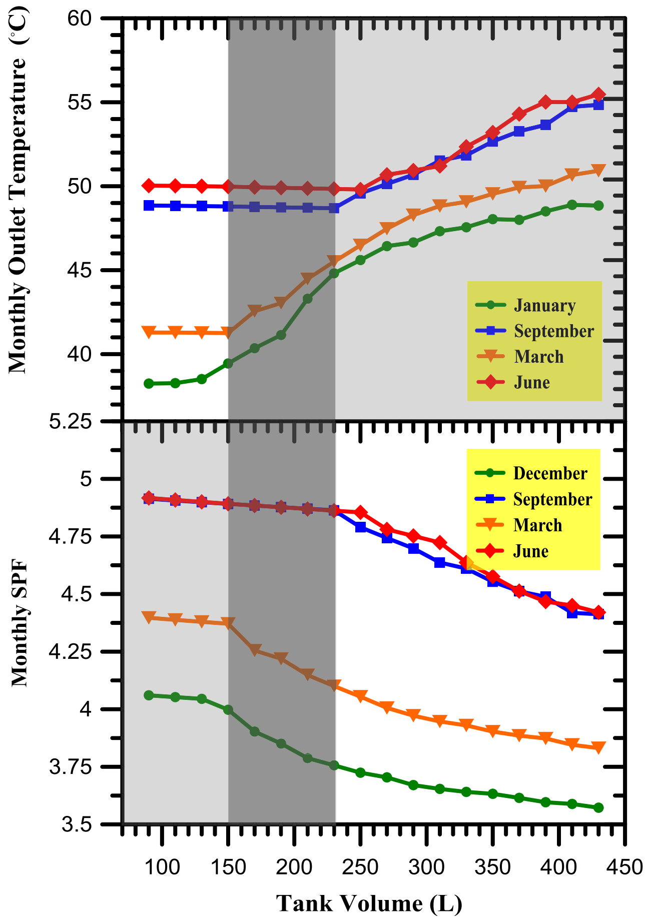

Fig. 8. Monthly seasonal performance factor and the outlet to load in Taipei during four months.

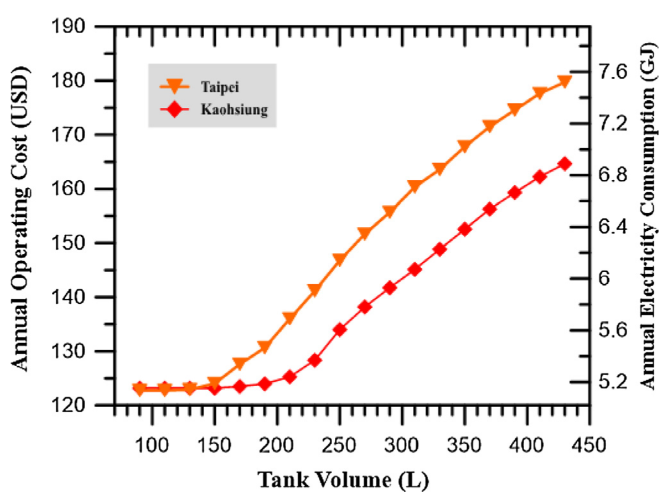

Fig. 9. Annual operating costs and annual electricity consumption levels of tanks of various volumes in Taipei and Kaohsiung.

the two aforementioned requirements, the appropriate volume of a DW tank ranges from 170 L to 290 L in Kaohsiung, as indicated by the region shaded in dark gray in Fig. 12. Fig. 13 shows the monthly SPF values for systems with various heat pump flow rates in Kaohsiung during different months. Fig. 14 shows the yearly SPF values for systems of various heat pump flow rates in Kaohsiung. In Kaohsiung, the yearly SPF achieves its highest value when the heat

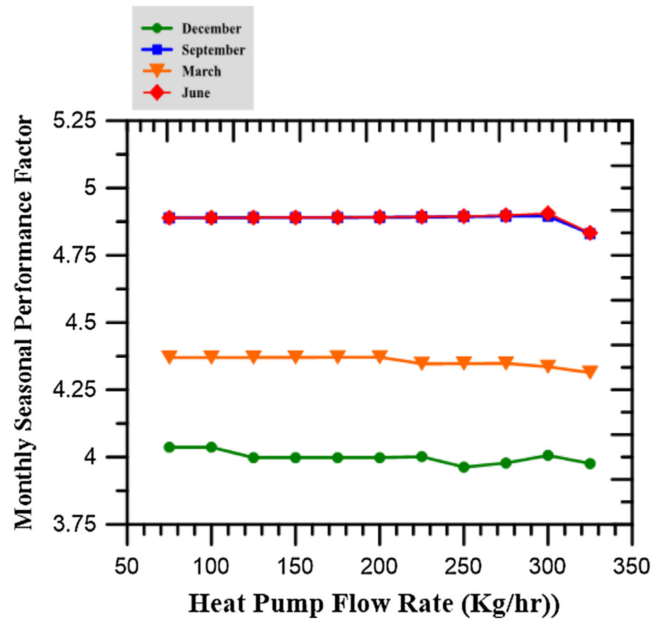

Fig. 10. Monthly seasonal performance factors for systems of various heat pump flow rates in Taipei during four months.

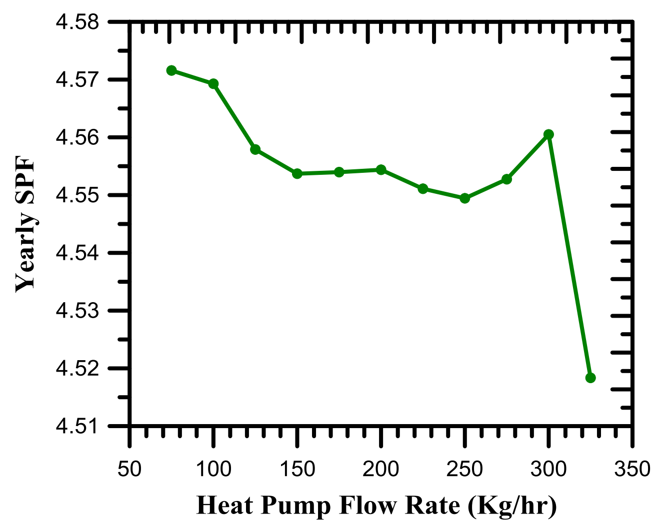

Fig. 11. Yearly seasonal performance factors for systems of various heat pump flow rates in Taipei.

pump flow rate is in the range of 275–300 kg/h, which is considered to be the appropriate range of heat pump flow rates. For Taipei, Fig. 15 presents the monthly SPF for systems of various DHW flow rates in four representative months and the yearly SPF values for systems of various DHW flow rates. Fig. 16 presents similar information for Kaohsiung. The results reveal that SPF decreases during the cold seasons, as typified by the months of December and March. These results agree with previous results. The shaded areas of Figs. 15(b) and 16(b) categorize four levels of SPF values related to civil water consumption for optimized dual-tank combisystems in Taipei and Kaohsiung. The optimal settings refer to previous results.

In this study, maximum values of SPF of the solar combisystem range from 4.4 to 5.4 in Kaohsiung with tropical climate, and from 4 to 4.9 in Taipei with subtropical climate. Compared with other literature, the SPF values of solar combisystem are 3.85 in Carcassonne, France with Mediterranean climate (Poppi et al., 2016), 3.16

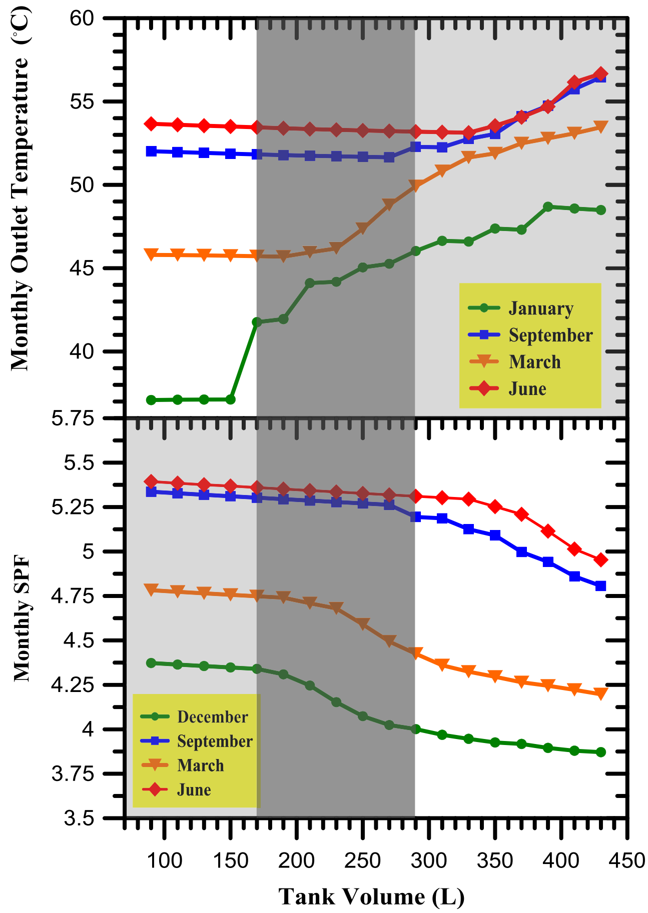

Fig. 12. Monthly seasonal performance factors and outlet temperatures to load in Kaohsiung during four months.

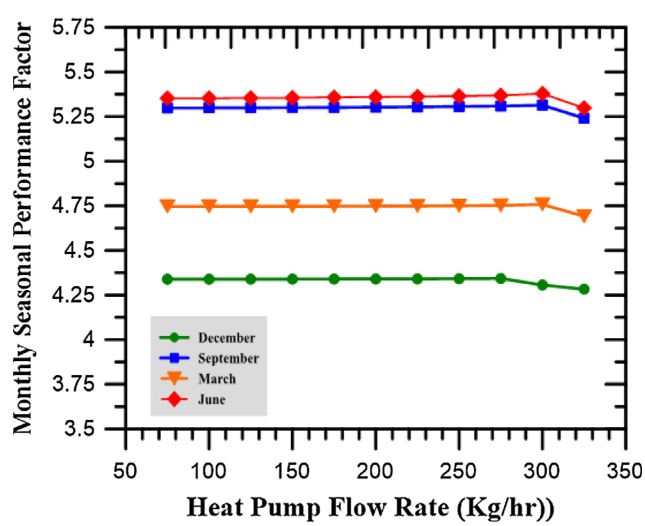

Fig. 13. Monthly seasonal performance factors for systems of various heat pump flow rates in Kaohsiung during four months.

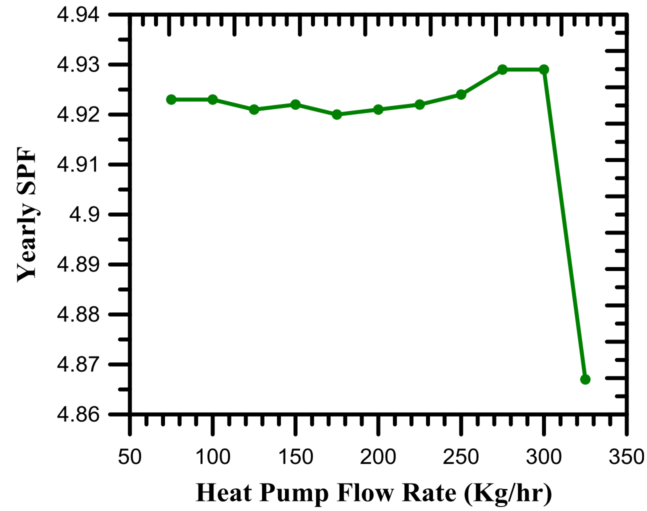

Fig. 14. Yearly seasonal performance factors for systems of various heat pump flow rates in Kaohsiung.

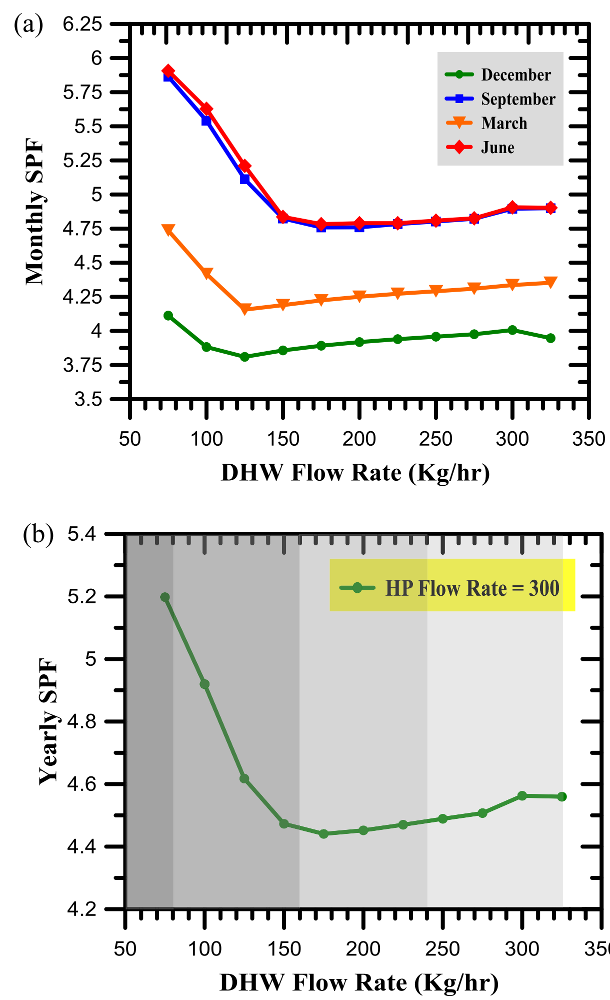

Fig. 15. Monthly and yearly seasonal performance factors for systems of various domestic hot water flow rates in Taipei.

in Zurich, Swiss with oceanic climate, and 2.5–2.9 in cold climate region (Bakirci and Yuksel, 2011). Most studies investigate the heating performance and thermal efficiency of solar combisystem under the cold weather condition or Mediterranean climate, rarely in warm regions. It is anticipated that SPF values are higher in warm regions than in cold regions. However, inappropriate hydraulic layouts of solar combisystems in warm region would lead to reduction of heating performance of SDHW and meanwhile increase of operating and equipment cost.

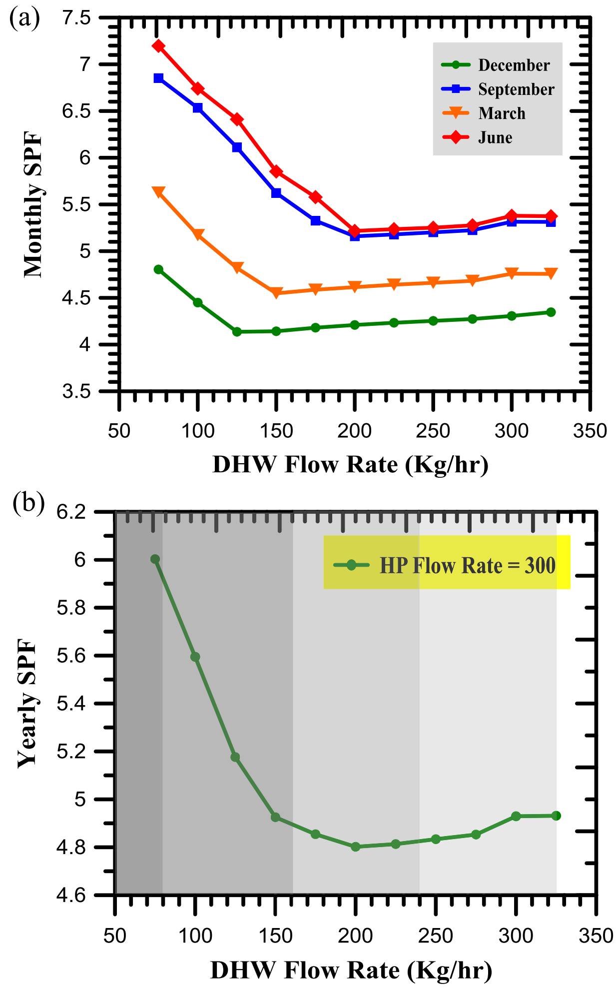

Fig. 16. Monthly and yearly seasonal performance factors for systems of various domestic hot water flow rates in Kaohsiung.

4.3. System comparisons

The overall energy values obtained from the TRNSYS simulations for each system are summarized in Table 1 for Taipei and in Table 2 for Kaohsiung. The energy entering the system comprises the solar energy collected and the electric loads for the pumps, heat pump, and auxiliary heaters, whereas the energy exiting the system comprises heated water at 50 °C and losses from the tanks to the surrounding environment.

In Taipei, a single-tank combisystem uses a small amount of electrical energy and obtains more solar energy than a comparable SDHW system. The installation of a heat pump in a DHW system with a single tank affects its capacity for solar energy collection.

Table 1
Overall simulation results for the three systems in Taipei.

System	SDHW	Combisystem with a single tank	Combisystem with dual tank
Auxiliary heater (GJ)	31.2	N/A	N/A
Pumps (GJ)	0.122	0.524	0.504
Heat pump (GJ)	N/A	7.12	5.41
Total electrical load (GJ)	31.322	7.644	5.914
Collected solar (GJ)	5.35	5.77	7.42
Tank losses (GJ)	2.08	1.61	1.182
SPF_{system}	1.1	3.92	4.36
SF (%)	15.5	18.8	19.8

Table 2
Overall simulation results for the three systems in Kaohsiung.

System	SDHW	Combisystem with a single tank	Combisystem with dual tanks
Auxiliary heater (GJ)	28.2	N/A	N/A
Pumps (GJ)	0.138	0.497	0.492
Heat pump (GJ)	N/A	6.21	4.88
Total electrical load (GJ)	28.338	6.7	5.372
Collected solar (GJ)	7.17	7.75	9.57
Tank losses (GJ)	2.07	1.62	1.522
SPF_{system}	1.18	4.31	4.83
SF (%)	21.5	26.3	28.3

Such a heat pump elevates the temperature of a large portion of the water inside the DW tank during operation. Therefore, the storage tank in the dual-tank combisystem increases the amount of collected solar heat in the dual-tank combisystem by a quantity approximately equal to the amount in the single-tank combisystem system (Table 1). This is due to the generally colder water temperature in the storage tank, which enhances collector efficiencies and solar collection run times. Although the dual-tank combisystem has two tanks and an additional 230 L of water in the system, it uses less electrical energy than does the single-tank combisystem because its heat pump consumes less energy and its tanks lose less energy. The DW tank in a dual-tank combisystem is much smaller than that in a single-tank combisystem; thus, the heat loss and energy consumption levels of the heat pump in the single-tank system are higher. In Taipei, the SPFs for the SDHW system, single-tank combisystem, and dual-tank combisystem are 1.1, 3.92, and 4.63, respectively. This demonstrates that, in Taipei, the heating capacity of the dual-tank combisystem is most efficient in terms of electrical consumption. The SFs are 15.5%, 18.8%, and 19.8% for the SDHW system, single-tank combisystem, and dual-tank combisystem, respectively.

The Kaohsiung region has more abundant solar irradiation than the Taipei region does; the incremental values of collected solar energy in Table 2 show that the contributions of solar energy to Kaohsiung's DHW systems were higher. One might anticipate reduced energy consumption for the auxiliary heater and heat pump in Kaohsiung. Despite an increase of solar thermal utilization in the two combisystems, the influences of heating capacities between the solar collector and heat pump are still significant. The SF of the single-tank combisystem is greater than that of the SDHW system. The dual-tank SC-HP DHW system collects more solar energy than the SDHW system does, and the corresponding value of the SF for the dual-tank combisystem is also higher than that for the SDHW system. Similarly, the values of SPF for the combisystems are evidently larger than that for the SDHW system. This reveals that the integration of the heat pump in the solar thermal water system improves the electrical efficiency of the DHW system.

Fig. 17 compares the normalized energy demands of single-tank solar combisystems in Taipei and Kaohsiung. The solar thermal energy in Kaohsiung contributes a significant portion of normalized energy demand for the DHW system during the summer months compared with that in Taipei. This is due to the higher levels of solar irradiation in Kaohsiung. However, the heat pump causes a larger portion of the normalized energy demand in Taipei, and even in summer months, the water heating contribution of the heat pump is more than 80% of the system's overall energy requirement. Fig. 18 compares the normalized energy demands of dual-tank solar combisystems in Taipei and Kaohsiung. In general, the storage tank in the dual-tank combisystem increases the overall thermal mass, and in conjunction with the heat pump, the system is able to collect and store more solar energy. In particular, the contribution of solar thermal energy to overall energy demand in

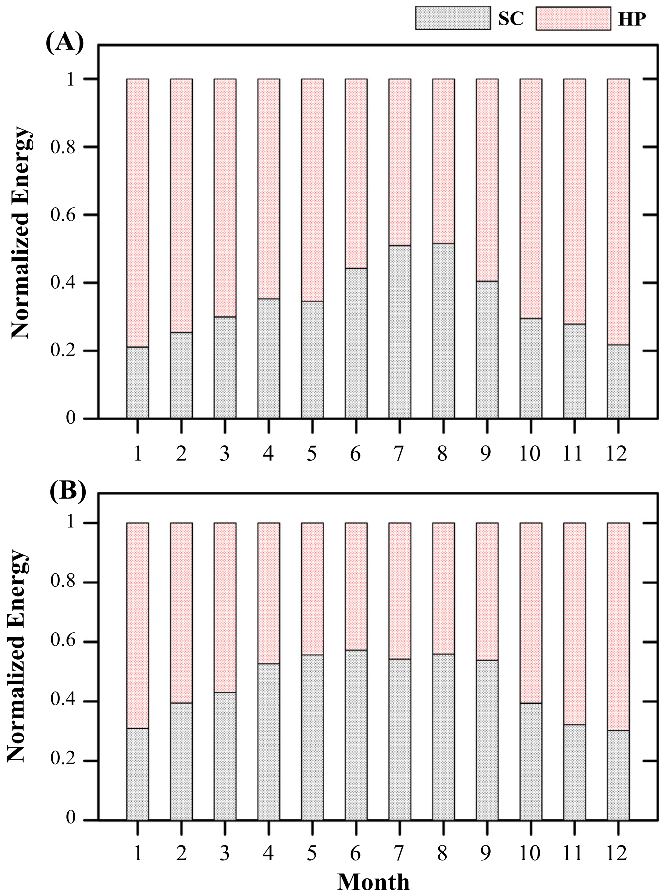

Fig. 17. Comparison of monthly energy requirements of single-tank solar combisystems in (A) Taipei and (B) Kaohsiung.

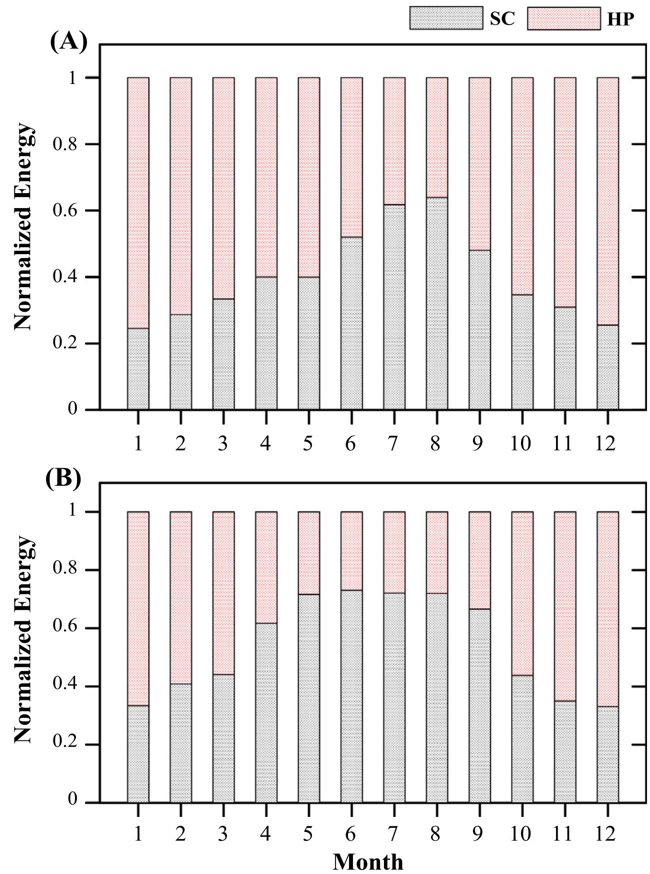

Fig. 18. Comparison of monthly energy requirements of dual-tank solar combisystems in (A) Taipei and (B) Kaohsiung.

Kaohsiung increases 16% in the summer months and increases 70% in winter months. The overall increase in the contribution of solar thermal energy to overall energy demand in Kaohsiung is 34%. The increase of solar thermal energy utilization in Taipei is significant in winter months such as October, November, December, January, and February. Increases in the contribution of solar thermal energy to overall energy demand are 117%, 27%, and 56% for winter months, summer months, and the whole year, respectively. In Taipei and Kaohsiung, particularly in the winter months, the addition of the storage tank in the solar combisystem substantially improves the contribution of solar thermal energy in terms of energy requirements. However, the heating performance of a DHW system in Taipei is still dominated by the heating capacity of the heat pump. This highlights the fact that, in Taipei, the overall energy demand depends on the heat pump. Fig. 19 shows the SPF of various heat pump flow rates with different system layouts in Taipei and Kaohsiung. In Taipei and Kaohsiung, the results revealed that SPF values of dual-tank combisystems are higher than those of single-tank combisystems for different heat pump flow rates, and furthermore, the SPF values of dual-tank combisystems are also higher than those of single-tank combisystems for different DHW flow rates, as shown in Fig. 20. This reveals that the combination of a heat pump and an additional tank in a DHW system not only improves the SF of the DHW system, but also enables the DHW system to achieve a higher SPF value.

Although technical analysis is necessary to this work, estimating realistic payback periods and gauging the economic feasibility of specific solar combisystems is also crucial in this study. The payback period is calculated by counting the number of years it will take to recover the cash invested in a project. To determine the payback period, the operating cost ($/year) and the equipment cost ($) should be known. In the paper, we would like to examine the payback period of SDHW system with regard to the replacement of conventional domestic hot water (DHW) system, such as electrical heater or gas-fired heater. The definition of effective payback period is a ratio of the equipment cost difference between SDHW and conventional DHW to the operational cost difference between SDHW and conventional DHW:

$$\text{payback period} = \frac{|\text{Equipment cost of SDHW system} - \text{Equipment cost of conventional DHW system}|}{|\text{Operating cost of SDHW system} - \text{Operating cost of conventional DHW system}|}.$$

Compared to a single-tank combisystem, a dual-tank combisystem has a lower operating cost and a higher SPF, as shown in Figs. 21 and 22. Notably, a dual-tank combisystem has a lower annual operating cost; the reduction of annual operating cost in Taipei is greater than that of in Kaohsiung, because the interference between heat pump and solar collector is serious in Taipei. However, a dual-tank combisystem has higher equipment cost than a single-tank combisystem. According to the Taiwan Power Company, the average electricity rate in 2014 was approximately 0.086 USD/kW-h. The retail price of a heat pump with a heating capacity of 7 kW was approximately 1500 USD, an additional DW tank was 460 USD and the pump was 60 USD. Based on these values and the total electrical energy consumption for each system, the annual operating costs and SPFs for the five DHW systems were gauged (Table 3). Even though a dual-tank combisystem has the lowest operating cost, the capital outlay for additional equipment is significant. The more components that are added to a system, the higher its initial cost is. For the Taipei region, the operating cost of a single-tank combisystem saves 508 USD annually compared

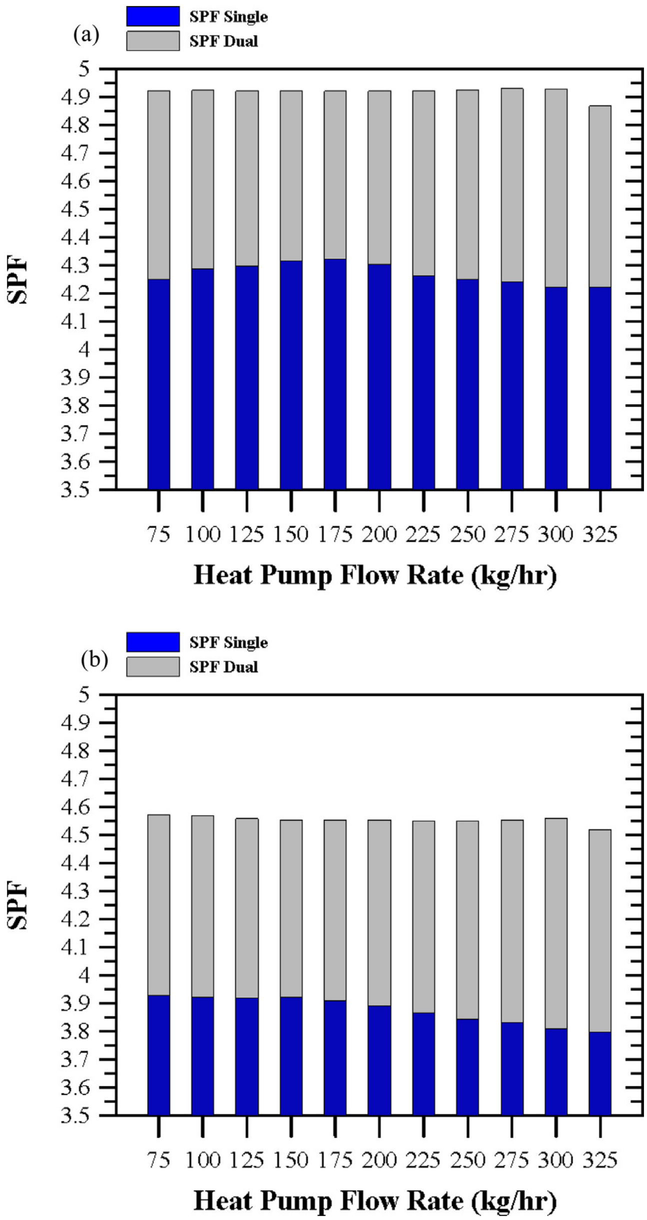

Fig. 19. Seasonal performance factors for systems of various heat pump flow rates with different system layouts in (a) Kaohsiung and (b) Taipei.

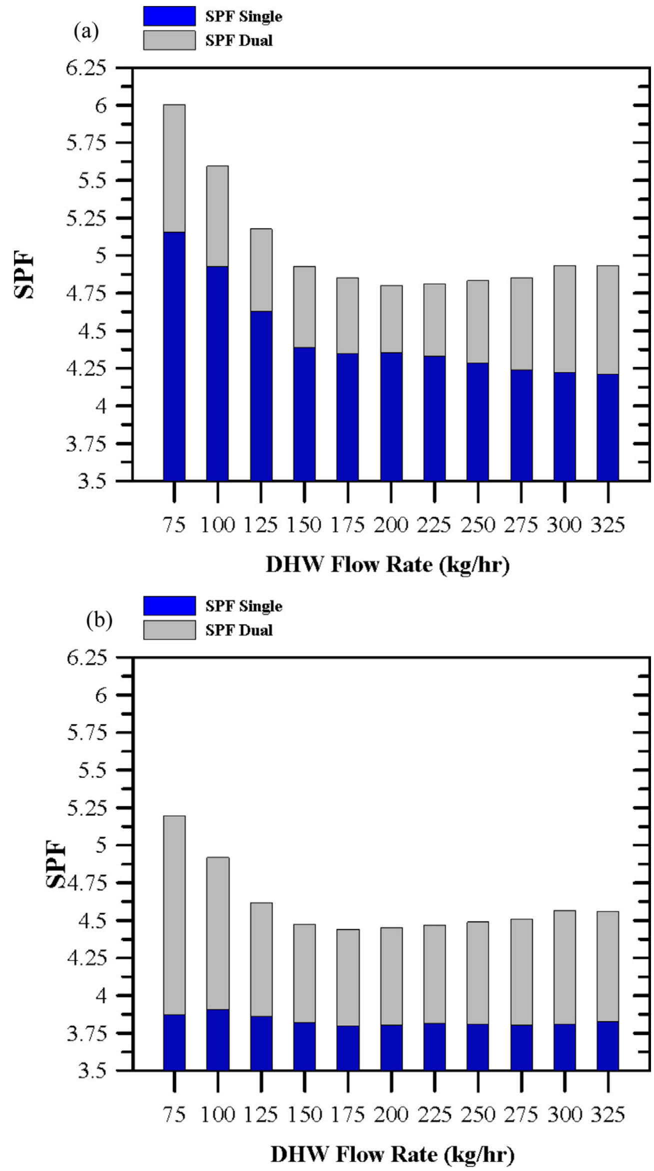

Fig. 20. Seasonal performance factors for systems of various domestic hot water flow rates with different system layouts in (a) Kaohsiung and (b) Taipei.

with a SDHW system. Fig. 23 illustrates payback periods in the context of a gas-fired heater. For the traditional SDHW, the payback periods relative to gas-fire heater are 5.83 years in Taipei and 8.27 years in Kaohsiung. In the solar combisystem, when the incremental capital price is considered, the payback periods of single-tank combisystems are roughly 3.79 and 4.59 years in Taipei and Kaohsiung, respectively. This calculation does not consider depreciation rates of the equipment, maintenance fees, and derivative expenses. Similarly, the payback periods of additional capital costs for dual-tank combisystems are 4.35 and 5.36 years. In Kaohsiung, however, annual operating costs for the five systems are notably lower than those in Taipei, and meanwhile the profit of solar DHW systems is not outstanding in Kaohsiung due to low water heating requirement. Accordingly, the payback periods of solar DHW systems are higher in Kaohsiung than in Taipei. In the context of the electrical heater, the payback periods for SDHW are 3.57 years in Taipei and 4.85 years in Kaohsiung, as shown in Fig. 24. It is apparent to reduce payback period in SDHW compared

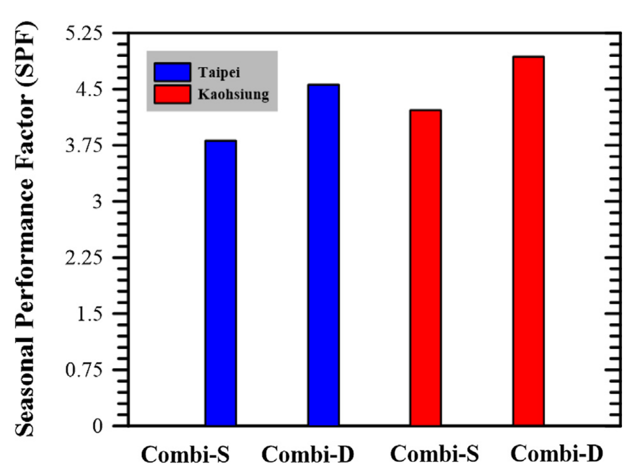

Fig. 21. Seasonal performance factor differences between single-tank and dual-tank combisystems in Taipei and Kaohsiung.

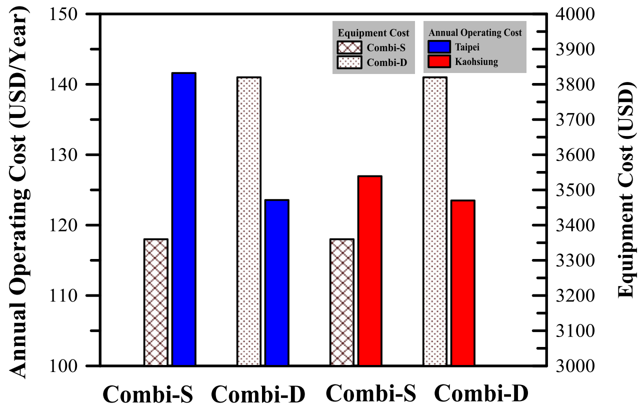

Fig. 22. Annual operating cost and equipment cost differences between single-tank and dual-tank combisystems in Taipei and Kaohsiung.

Table 3
Annual operating cost and system cost for three SDHW systems.

	Electrical Heater	Gas heater	SDHW	Combi-Single tank	Combi-Dual tank
Taipei					
SPF	0.88	N/A	1.11	3.81	4.56
Annual operating COST	874.00	830.00	650.00	141.61	123.57
Kaohsiung					
SPF	0.842	N/A	1.20	4.22	4.93
Annual operating COST	734.00	696.00	569.00	126.96	123.50

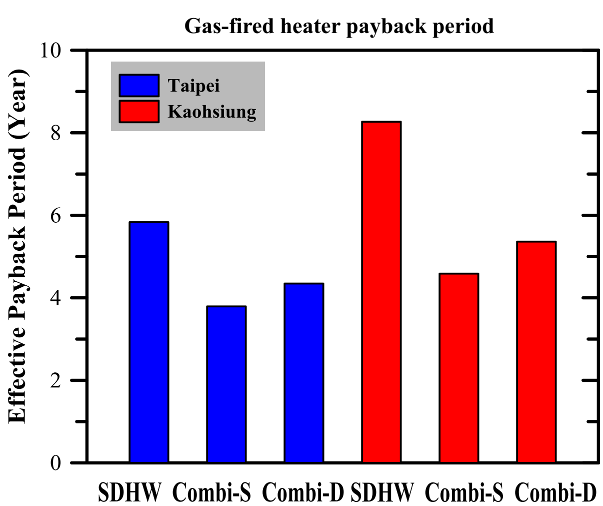

Fig. 23. Payback periods (relative to gas heaters) for three different types of domestic hot water systems in Taipei and Kaohsiung.

to these relative to gas-fired heater. Compared with the electrical heater, the payback periods for the single- and dual-tank solar combisystems are 3.89 and 4.62, respectively, in Taipei, and 4.59 and 5.36, respectively, in Kaohsiung. The payback period is an essential indicator for the consumer making the final design decision. A solar combisystem with a single tank is evidently economically beneficial and affordable, but not technically efficient and optimal in Taiwan. When one must convince consumers to invest in the installation of new equipment, the maximal payback period is 5 years. The payback periods of single-tank combisystems and dual-tank combisystems are shorter than 5 years in Taipei and the payback period of a single-tank combisystem is shorter than 5 years in Kaohsiung when compared with a gas-fired hot water system, as shown in Fig. 23. The payback periods of all DHW systems are shorter than 5 years in the context of an electrical heater, as shown in Fig. 24. The dual-tank solar combisystem is superior in terms of system efficiency and the single-tank solar combisystem is superior in terms of payback period. Therefore, appropriate incentive plans and regulatory approaches are necessary for the development of SC-HP DHWs. The support of public opinion is still required.

Table 4
Setting parameters of validated model and experimental apparatus.

Parameter	Value	Unit
Solar collector		
Collector area	3.84	m^2
Intercept efficiency	0.7	N/A
Efficiency slop	13	kJ/h m^2 K
Efficiency curvature	0.05	kJ/h m^2 K^2
Type	Flat plate	N/A
Temperature controller of solar collector loop		
Upper dead band dT	7	°C
Lower dead band dT	3	°C
Thermal storage tank		
Initial nodal temperature	25	°C
Tank volume	460	L
Number of nodes	3	N/A
Material	304 stainless steel	N/A
Pump		
Maximum flow rate	4.8	kg/min
Maximum power	0.37	kW
Heat pump		
Rated compressor power	1.7	kW
Rated heat capacity	7	kW
Total air flow rate	717	L/s
Blower power	662	kJ/h
Refrigerant	R410A	N/A
Temperature controller of heat pump loop		
Set point temperature	55	°C
High limit monitoring temperature	70	°C
Turn on temperature difference	5	°C
Turn off temperature difference	0	°C

5. Conclusions

In this study, comparisons were drawn between simulations and experiments regarding three different DHW systems. The parameters of TRNSYS modules were adjusted to bring the numerical results into accurate agreement with the experimental results. Regarding the heat pump modules, the Type 938 module was more accurate because it calculates the influence of relative humidity on heat transfer. After refinements, the simulations of SC-HP DHW systems were consistent with physical experimental results.

The combination of a solar collector and a heat pump is technically favorable for improving the overall efficiency of a DHW system. However, the addition of a heat pump to an SDHW system raises the capital cost and prolongs the payback period. A combined solar collector and heat pump (SC-HP) DHW system can prevent inconveniences caused by intermittent solar radiation, but from the user perspective, saving money on electricity bills consistently outweighs any improvement to the overall efficiency of a DHW system. The belief that combined SC-HP DHW systems are more efficient and more advantageous than conventional SDHW or heat pump hot water systems is debated among consumers in Taiwan.

The present study analyzed and compared performance levels for one conventional SDHW system and two combined SC-HP DHW systems in terms of electricity demand, solar thermal contribution, the optimal ranges of system settings, SPF, and payback

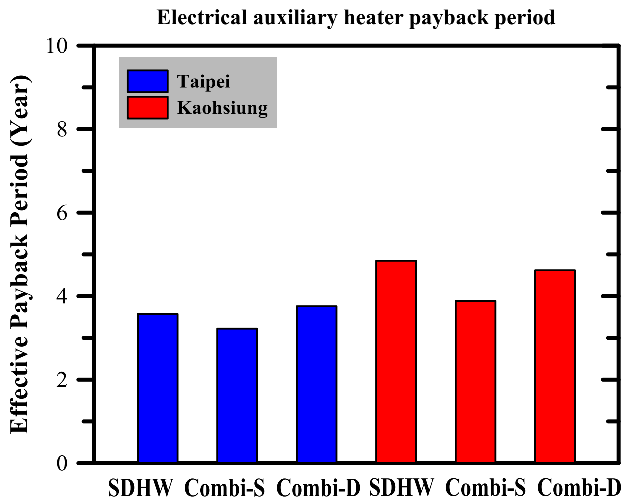

Fig. 24. Payback periods (relative to electric heaters) for three different types of domestic hot water systems in Taipei and Kaohsiung.

period. Three systems were defined and modeled according to state-of-the-art commercial systems in Taiwan: a SDHW system (with auxiliary electrical heater), a combined solar collector and heat pump system with a single tank, and a combined solar collector and heat pump system with dual tanks. Regarding the effect of climate conditions, two metropolitan cities in Taiwan were simulated; Taipei represented subtropical cities, and Kaohsiung represented tropical cities. Relatively lower solar irradiation in Taipei caused serious interference between the solar collector and heat pump in the solar combisystem with a single tank. With the addition of a secondary storage tank, the interference of heating performance was curtailed in the dual-tank combisystem, which showed benefits for increased seasonal SF, increased SPF, and decreased electrical load. In addition, simulation results demonstrated that the contributions of solar thermal energy to DHW systems are more significant in Kaohsiung than in Taipei because of climate conditions and geographic location. Kaohsiung had low overall electrical loads and high heat losses from tanks during the entire simulation period. The solar combisystems with dual tanks were superior to the other two types based on identical water delivery temperature, water draw schedule, and environmental conditions.

According to current electricity rates and equipment prices, the payback periods for one conventional SDHW system and two combined SC-HP DHW systems were determined. The annual operating costs for combined SC-HP DHW systems are essentially lower than those for an SDHW system. However, when the capital costs are considered, the payback periods of the combined SC-HP DHW systems are more attractive in Taipei than they are in Kaohsiung, and the single-tank system is more cost-effective than the dual-tank system. The dual-tank solar combisystem is more efficient and the single-tank solar combisystem is preferable in terms of payback period. The economically optimal choice conflicts with the technically optimal choice. This suggests that computer simulation is crucial for estimating the performance of SC-HP DHW systems and for optimizing hot water systems economically and technically according to climate conditions and geographic locations.

Acknowledgements

This research was partially supported by the Ministry of Science and Technology under Grant No. MOST 104-2228-E-006 -012, and by the Bureau of Energy and Ministry of Economic Affairs, under Grant No. 105-D0303, Republic of China. Computer time and numerical packages provided by the Energy Research Center, National Cheng Kung University, Taiwan, are gratefully acknowledged.

References

Asaee, S.R., Ugursal, V.I., Beausoleil-Morrison, I., 2017. Techno-economic assessment of solar assisted heat pump system retrofit in the Canadian housing stock. Appl. Energy 190, 439–452.

Awani, S., Kooli, S., Chargui, R., Guizani, A., 2017. Numerical and experimental study of a closed loop for ground heat exchanger coupled with heat pump system and a solar collector for heating a glass greenhouse in north of Tunisia. Int. J. Refrig. 76, 328–341.

Bakirci, K., Yuksel, B., 2011. Experimental thermal performance of a solar source heat-pump system for residential heating in cold climate region. Appl. Therm. Eng. 31, 1508–1518.

Banister, C.J., Collins, M.R., 2015. Development and performance of a dual tank solar-assisted heat pump system. Appl. Energy 149, 125–132.

Bertram, E., 2014. Solar assisted heat pump systems with ground heat exchanger – simulation studies. Energy Procedia 48, 505–514.

Buker, M.S., Riffat, S.B., 2016. Preliminary performance test of a combined solar thermal roof system with heat pump for buildings. Energy Procedia 91, 421–431.

Buker Mahmut, S., Riffat, S.B., 2016. Solar assisted heat pump systems for low temperature water heating applications: a systematic review. Renew. Sustain. Energy Rev. 55, 399–413.

Bureau of Energy, Ministry of Economic Affairs, 2015. Energy Statistical data Handbook 2014.

Carbonell, D., Haller, M.Y., Frank, E., 2014. Potential benefit of combining heat pumps with solar thermal for heating and domestic hot water preparation. Energy Procedia 57, 2656–2665.

Carbonell, D., Haller, M.Y., Philippen, D., Frank, E., 2014. Simulations of combined solar thermal and heat pump systems for domestic hot water and space heating. Energy Procedia 48, 524–534.

Chang, K.-C., Lee, T.-S., Lin, W.-M., Chung, K.-M., 2008. Outlook for solar water heaters in Taiwan. Energy Policy 36, 66–72.

Chaturvedi, S.K., Gagrani, V.D., Abdel-Salam, T.M., 2014. Solar-assisted heat pump – a sustainable system for low-temperature water heating applications. Energy Convers. Manage. 77, 550–557.

Chen, F., Lu, S.-M., Chi-Chuan, W., Chang, Y.-L., 2008. Promotion strategies for renewable energy in Taiwan. Renew. Sustain. Energy Rev. 12, 1681–1691.

Chow, T.T., Pei, G., Fong, K.F., Lin, Z., Chan, A.L.S., He, M., 2010. Modeling and application of direct-expansion solar-assisted heat pump for water heating in subtropical Hong Kong. Appl. Energy 87, 643–649.

Chu, J., Cruickshank, C.A., 2014. Solar-assisted heat pump systems: a review of existing studies and their applicability to the Canadian residential sector. J. Sol. Energy Eng. 136, 041013.

Deng, S., Dai, Y.J., Wang, R.Z., 2013. Performance optimization and analysis of solar combi-system with carbon dioxide heat pump. Sol. Energy 98 (Part C), 212–225.

Dott, R., Genkinger, A., Afjei, T., 2012. System evaluation of combined solar & heat pump systems. Energy Procedia 30, 562–570.

Duffie, J.A.B.W., 1991. Solar Engineering of Thermal Processes. Wiley, New York, USA.

Emmi, G., Zarrella, A., De Carli, M., Galgaro, A., 2015. An analysis of solar assisted ground source heat pumps in cold climates. Energy Convers. Manage. 106, 660–675.

Haller, M.Y., Haberl, R., Mojic, I., Frank, E., 2014. Hydraulic integration and control of heat pump and combi-storage: same components, big differences. Energy Procedia 48, 571–580.

Hawlader, M.N.A., Chou, S.K., Ullah, M.Z., 2001. The performance of a solar assisted heat pump water heating system. Appl. Therm. Eng. 21, 1049–1065.

Jradi, M., Veje, C., Jørgensen, B.N., 2017. Performance analysis of a soil-based thermal energy storage system using solar-driven air-source heat pump for Danish buildings sector. Appl. Therm. Eng. 114, 360–373.

Kjellsson, E., Hellström, G., Perers, B., 2010. Optimization of systems with the combination of ground-source heat pump and solar collectors in dwellings. Energy 35, 2667–2673.

Kong, X.Q., Li, Y., Lin, L., Yang, Y.G., 2017. Modeling evaluation of a direct-expansion solar-assisted heat pump water heater using R410A. Int. J. Refrig. 76, 136–146.

Kumar, K.V., Paradeshi, L., Srinivas, M., Jayaraj, S., 2016. Parametric studies of a simple direct expansion solar assisted heat pump using ANN and GA. Energy Procedia 90, 625–634.

Le Roux, W.G., 2016. Optimum tilt and azimuth angles for fixed solar collectors in South Africa using measured data. Renew. Energy 96 (Part A), 603–612.

Lerch, W., Heinz, A., Heimrath, R., 2015. Direct use of solar energy as heat source for a heat pump in comparison to a conventional parallel solar air heat pump system. Energy Build. 100, 34–42.

Li, Y.W., Wang, R.Z., Wu, J.Y., Xu, Y.X., 2007. Experimental performance analysis and optimization of a direct expansion solar-assisted heat pump water heater. Energy 32, 1361–1374.

Li, H., Sun, L., Zhang, Y., 2014. Performance investigation of a combined solar thermal heat pump heating system. Appl. Therm. Eng. 71, 460–468.

Lin, H.T., Huang, K.T., 2005. The research and application of typical meteorological years of Taiwan. J. Archit. 53, 79–94.

Lin, W.M., Chang, K.C., Chung, K.M., 2015. Payback period for residential solar water heaters in Taiwan. Renew. Sustain. Energy Rev. 41, 901–906.
Liu, Y., Ma, J., Zhou, G., Zhang, C., Wan, W., 2016. Performance of a solar air composite heat source heat pump system. Renew. Energy 87 (Part 3), 1053–1058.
Liu, B.Y.H., Jordan, R.C., 1960. The interrelationship and characteristic distribution of direct, diffuse and total solar radiation. Sol. Energy 4, 1–19.
Liu, L., Zhu, N., Zhao, J., 2016. Thermal equilibrium research of solar seasonal storage system coupling with ground-source heat pump. Energy 99, 83–90.
Lund, P.D., 2005. Sizing and applicability considerations of solar combisystems. Sol. Energy 78, 59–71.
Mohanraj, M., Jayaraj, S., Muraleedharan, C., 2012. Applications of artificial neural networks for refrigeration, air-conditioning and heat pump systems—a review. Renew. Sustain. Energy Rev. 16, 1340–1358.
Moreno-Rodríguez, A., González-Gil, A., Izquierdo, M., Garcia-Hernando, N., 2012. Theoretical model and experimental validation of a direct-expansion solar assisted heat pump for domestic hot water applications. Energy 45, 704–715.
Panaras, G., Mathioulakis, E., Belessiotis, V., 2013. Investigation of the performance of a combined solar thermal heat pump hot water system. Sol. Energy 93, 169–182.
Poppi, S., Bales, C., Haller, M.Y., Heinz, A., 2016. Influence of boundary conditions and component size on electricity demand in solar thermal and heat pump combisystems. Appl. Energy 162, 1062–1073.
Poppi, S., Bales, C., Heinz, A., Hengel, F., Chèze, D., Mojic, I., et al., 2016. Analysis of system improvements in solar thermal and air source heat pump combisystems. Appl. Energy 173, 606–623.
Qu, S., Ma, F., Ji, R., Wang, D., Yang, L., 2015. System design and energy performance of a solar heat pump heating system with dual-tank latent heat storage. Energy Build. 105, 294–301.
Rad, F.M., Fung, A.S., Leong, W.H., 2013. Feasibility of combined solar thermal and ground source heat pump systems in cold climate, Canada. Energy Build. 61, 224–232.
Reda, F., 2017. Solar assisted ground source heat pump solutions effective energy flows climate management.
Sterling, S.J., Collins, M.R., 2012. Feasibility analysis of an indirect heat pump assisted solar domestic hot water system. Appl. Energy 93, 11–17.
TRNSYS, 2012. A Transient System Simulation Program: V17.01.0025. Solar Energy Lab, University of Wisconsin-Madison, USA.
Tzivanidis, C., Bellos, E., Mitsopoulos, G., Antonopoulos, K.A., Delis, A., 2016. Energetic and financial evaluation of a solar assisted heat pump heating system with other usual heating systems in Athens. Appl. Therm. Eng. 106, 87–97.
Wang, X., Zheng, M., Zhang, W., Zhang, S., Yang, T., 2010. Experimental study of a solar-assisted ground-coupled heat pump system with solar seasonal thermal storage in severe cold areas. Energy Build. 42, 2104–2110.
Wu, J.H., Huang, Y.H., 2006. Renewable energy perspectives and support mechanisms in Taiwan. Renew. Energy 31, 1718–1732.
Xi, C., Hongxing, Y., Lin, L., Jinggang, W., Wei, L., 2011. Experimental studies on a ground coupled heat pump with solar thermal collectors for space heating. Energy 36, 5292–5300.
Zhu, J., Li, D., Zhao, S., 2015. Study on application of solar water heat pump for building in China. Procedia Eng. 121, 1200–1207.